Influence of Copper Nanoparticles Concentration on the Properties of Poly(vinylidene fluoride)/Cu Nanoparticles Nanocomposite Films

B. Jaleh · P. Fakhri · M. Noroozi · N. Muensit

Abstract In this study, the nanocomposite films of polyvinylidene fluoride/copper nanoparticles were prepared by mixing of copper nanoparticles in a solution of dimethylformamide and polyvinylidene fluoride. The prepared nanocomposites were investigated by fourier transform infrared spectroscopy and X-ray diffraction techniques, showed an obvious α- to β-phase transformation compared to pure PVDF. Scanning electron microscope micrographs showed spherulitic crystal structure of PVDF. The spherulitic morphology of the pure PVDF is maintained for the PVDF nanocomposites; the size of the spherulites decreased by increasing weight fraction of copper nanoparticles. The optical band gap values deduced from the UV–Visible absorption spectra were found to reduce from 4.77 eV in pure PVDF to 3.2 eV after embedding 1 wt% of copper nanoparticles. The surface resistivity values were decreased with increasing copper nanoparticles content. Thermal stability of the nanocomposites was studied by thermogravimetric analysis (TGA). TGA curves showed that nanocomposite films have higher resistance to thermal degradation compared to pure PVDF.

Keywords PVDF · Copper nanoparticles · β-Phase · Thermal stability

B. Jaleh (✉) · P. Fakhri
Department of Physics, Bu Ali Sina University, Hamedan, Iran
e-mail: bkjaleh@yahoo.com; jaleh@basu.ac.ir

M. Noroozi
Faculty of Chemistry, Bu Ali Sina University, Hamedan, Iran

N. Muensit
Department of Physics, NANOTEC Center of Excellence at Prince of Songkla University, Songkla, Thailand

1 Introduction

Polyvinylidene fluoride (PVDF) is a widely studied semi-crystalline polymer due to its piezoelectric and pyroelectric properties [1]. Consequently, PVDF finds widespread applications in transducers, sensors, actuators and MEMS [2–4]. Piezoelectric properties of PVDF are strongly related to its crystalline structure [5]. PVDF crystallizes into five different polymorphs which include α, β, γ, δ, and ε, depending upon crystallization conditions [6]. The α-phase is the most common and stable polymorph of PVDF [7] with TGTG chain conformation and can be produced by cooling from the melt. The β-phase presents TTTT planar zigzag structure and γ-phase has T3GT3G conformation [8]. The δ and ε polymorphs are polar and antipolar analogues of the α and γ forms, respectively [9]. Among all the PVDF polymorphs, the β-phase is responsible for piezo- and pyroelectric properties of PVDF [10]. Unfortunately, the β-phase is thermodynamically unstable, due to the intensive repulsion developed between the adjacent CF_2 groups [11]. PVDF films often form the α-phase and β-phase can be obtained by stretching, applying high pressure and high electrical field to the α-phase [12]. Recently, the combination of PVDF with nanomaterials to form polymer nanocomposites has been an attractive approach to promote β-polymorph within the polymer and, therefore, improve its piezoelectricity. The effects of the addition of nanoclays, graphene sheets and MWNTs on PVDF crystalline structure have been studied [13–15]. A similar polymorph change has also been observed with other PVDF nanocomposites prepared from silver [16] and gold [17] nanoparticles. In general, the high cost of these nanomaterials precludes their extensive use in industrial sectors. In the present work, copper nanoparticles (Cu-NPs) were added into PVDF with two purposes. The first one is to investigate of the effect of Cu-NPs addition on

the polymorph changing of PVDF; the second one is to study the effect of Cu-NPs on the optical, electrical and thermal properties of PVDF.

Cu-NPs, due to their interesting electrical, optical and thermal properties and less cost than other noble metal such as silver and gold have attracted a lot of interest. As reported in literature, Cu-NPs are employed to improve the thermal stability [18] and electrical conductivity [19] of materials.

In this work, Cu-NPs were prepared with chemical reduction method. Nanocomposites of PVDF/Cu were prepared by a solution mixing technique for different Cu-NPs concentrations. The prepared films were studied by FTIR, XRD, SEM, UV–Vis, two-probe and TGA analysis. The α- to β-phase transition, spherulites size and band gap reduction, conductivity enhancement and increasing the thermal stability of the nanocomposite films were observed in comparison to the pure PVDF film.

## 2 Experimental

2.1 Materials

PVDF (Mw = 534,000), in powder form, was purchased from Sigma Aldrich. Dimethyl formamide (DMF) (Merck) of purity 99.5% was used as solvent. Cu-NPs were synthesized by following the procedures described below.

2.2 Synthesis of Cu-NPs

Cu-NPs are synthesized by the reaction of copper (II) sulfate pentahydrate ($CuSO_4 \cdot 5H_2O$) with sodium borohydride via wet method [20, 21]. Briefly, in the first stage, 200 mL of sodium hydroxide solution (NaOH) with a concentration of 2 M is added slowly with stirring to 100 mL copper sulphate solution with a concentration of 2 M. The solution temperature was raised to 80 °C with vigorous stirring [20, 21]. Copper hydroxide ($Cu(OH)_x$) and copper oxide (CuO_x) are formed and deposited as sediments. Then, the sediments are filtered and recovered. Distilled water and glucose are added to obtained precipitate and agitated until the color of the solution changed into dark red. Glycine (NH_2–CH_2–COOH) is added to the aqueous solution and this solution was placed into an ultrasonic bath. Then 100 mL of sodium borohydride solution (24 M), as a reducing agent, is added to solution drop by drop. The mixture is filtered, washed with distilled water and dried at 110 °C in an inert atmosphere (N_2). The molar ratio of the mixture Cu^{+2}:NaOH:Glycine:$NaBH_4$ are 1:2:1:12, respectively [20, 21].

2.3 Preparation of the Nanocomposites

PVDF solution was prepared by dissolving the PVDF powder into DMF with a mass ratio of 10/90 and stirred for 3 h to obtain a homogeneous and transparent solution. In order to get a homogeneous dispersion of the Cu-NPs inside the polymeric matrix, the following procedure was applied: first, the desired amount of Cu-NPs and DMF were mixed then this mixture was placed in an ultrasound bath for 5 h to ensure that the nanoparticles were well dispersed in the DMF and to avoid aggregates; then the corresponding amount of PVDF solution was added. The obtained mixture was placed in a stirrer to complete dissolution of the polymer and then was dried on a petri dish inside the oven for 2 h at 120 °C to ensure the complete crystallization of the nanocomposites and complete removal of the solvent. To prevent the oxidation of Cu-NPs, these processes were carried out under nitrogen atmosphere. The mass ratio of Cu to PVDF in the mixture was varied from 0.05, 0.1, 0.5 to 1. The flowcharts for nanoparticle synthesis and nanocomposite preparation were presented, respectively in Fig. 1a and b.
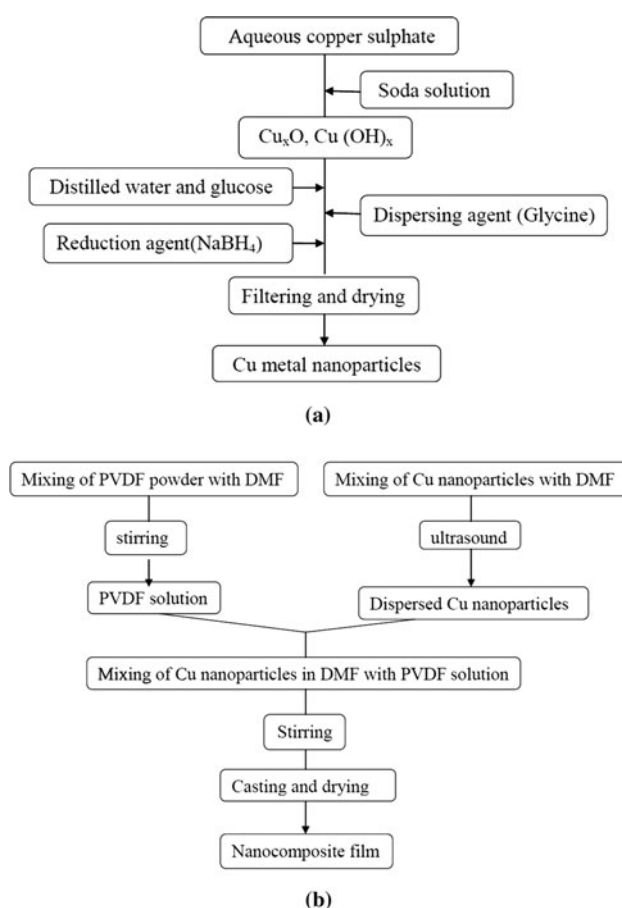
Fig. 1 Flowchart of: **a** nanoparticle synthesis and **b** nanocomposite preparation

2.4 Characterization

The crystalline phase of the PVDF in each sample was determined by FTIR spectroscopy (Shimadzu, 8000 series) at room temperature. The UV–visible measurements were performed at room temperature by a Perkin Elmer 550ES from 300 to 800 cm^{-1} with a resolution of 1 nm. X-ray diffraction measurements were performed with a Philips powder diffractometer type PW 1373 goniometer. It was equipped with a graphite monochromator crystal. The X-ray wavelength was 1.5405 Å and the diffraction patterns were recorded in the 2θ range (10–60) with scanning speed of 2°/min. Morphology and particle dispersion was investigated by Scanning electron microscopy (SEM) (Cam scan MV2300) and Transmission electron microscopy (TEM) (Philips EM208S transmission electron microscope operating at an acceleration voltage of 100 kV). Thermogravimetric analysis (TGA) was performed using a Perkin Elmer system. The sample was heated under nitrogen atmosphere (70 cm^3 min^{-1}) at a rate of 10 °C min^{-1} from 200 to 600 °C. The electrical conductivity was measured with the two-probe method with an electrometer.

3 Results and Discussion

3.1 TEM

Figure 2a, b, and c shows the TEM images of Cu-NPs in different scales. It is observed that the particles are nanosized and approximately spherical. The mean diameter of the Cu-NPs is 25 nm.

3.2 FTIR Spectroscopy

Figure 3 shows the FTIR spectrums of the pure PVDF and PVDF/Cu nanocomposites with different concentrations of Cu. According to literature, the α-phase shows the characteristic absorption bands at 975 cm^{-1} (CH$_2$ twisting), 796 cm^{-1} (CH$_2$ rocking), 763 and 615 cm^{-1} (CF$_2$ bending and skeletal bending), 532 cm^{-1} (CF$_2$ bending) and 489 cm^{-1} (CF$_2$ bending) [6, 7] while β-polymorph has peaks at 510 and 840 cm^{-1} [6, 7]. The significant differences between FTIR spectra of pure PVDF and PVDF nanocomposites are the decreasing intensity of the vibration modes characteristic for α-phase and the appearance and increase of new vibration modes characteristic for β-phase (at 510 and 840 cm^{-1}). The FTIR spectroscopy is a suitable technique for quantitative determination of PVDF crystalline polymorphs [5]. The relative amount of β-phase was calculated using the following equation:
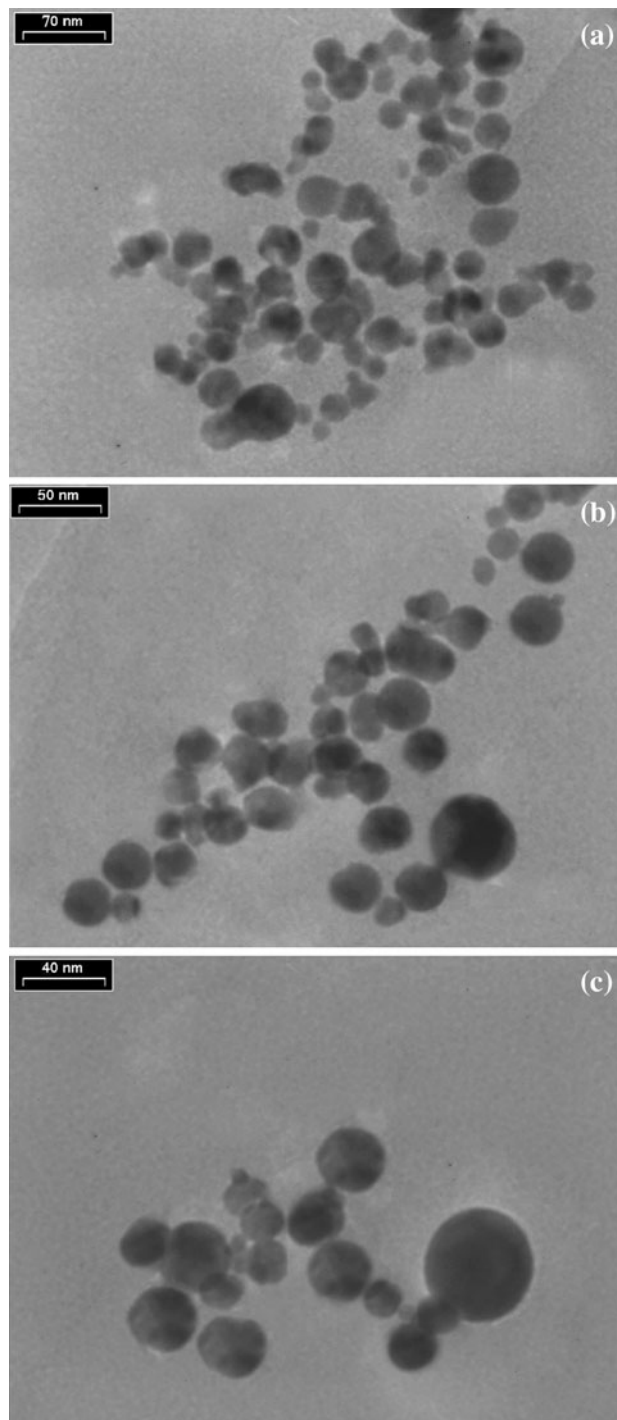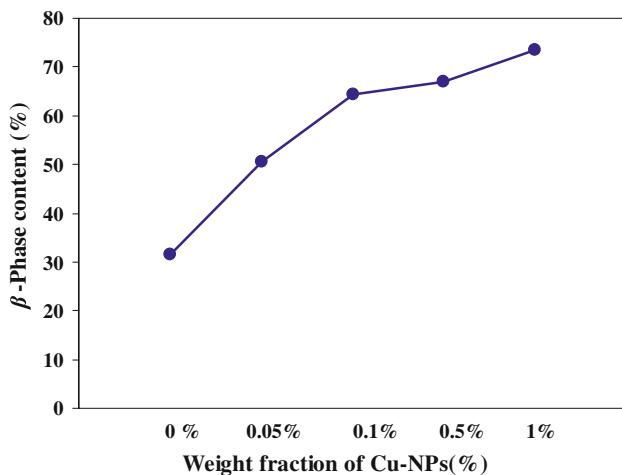

Fig. 2 TEM images of the Cu-NPs produced by chemical reduction

$$F(\beta) = \frac{X_\beta}{X_\beta + X_\alpha} = \frac{A_\beta}{(K_\alpha/K_\beta)A_\beta + A_\alpha} \tag{1}$$

where, $F(\beta)$ represents the β-phase content; A_α and A_β the absorbencies at 763 and 840 cm^{-1}, corresponding to the α- and β-phase, respectively; K_α and K_β are the absorption coefficients at the respective wave number and X_α and X_β are the degree of crystallinity of each phase. The value of
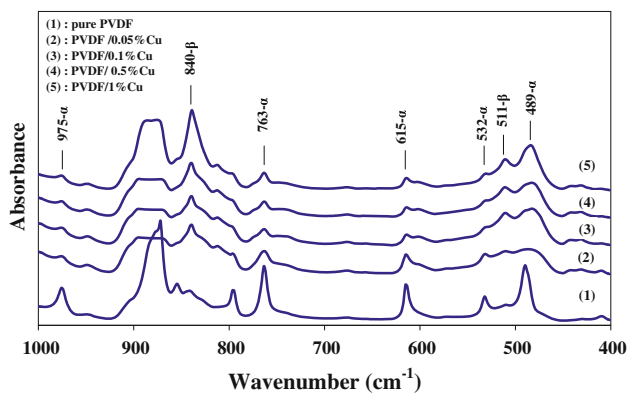
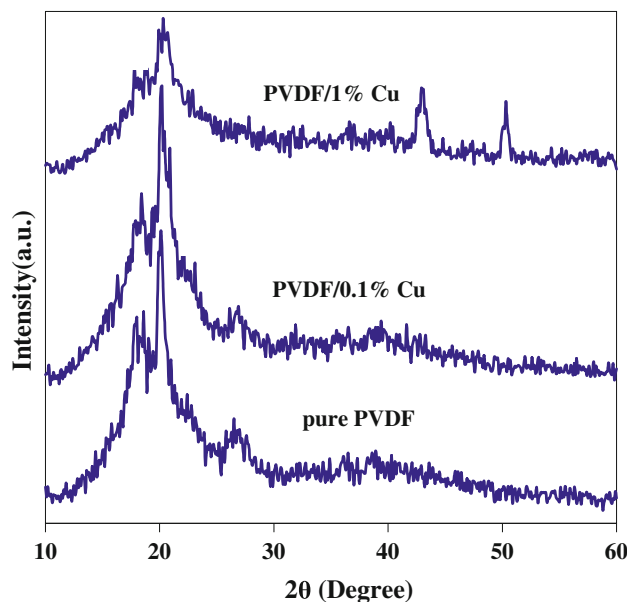**Fig. 3** FTIR spectra of PVDF and PVDF/Cu nanocomposites with different copper nanoparticle concentrations

Fig. 5 XRD patterns of pure PVDF and PVDF/Cu nanocomposites

Fig. 4 β-Phase content of PVDF and PVDF/Cu nanocomposites with different copper nanoparticle concentrations

K_α is 6.1×10^4 and K_β is 7.7×10^4 cm^2/mol [5]. The percentage of β-phase for pure PVDF and PVDF/Cu nanocomposites are shown in Fig. 4. It is observed that the β-phase content is increased as compared to that of pure PVDF. The amounts of 73% β for PVDF/1% Cu film were resulted, which is a good achievement. The changes in the FTIR spectra of the nanocomposite films can be explained by the electrostatic interaction between the surface charge of the Cu-NPs and CF electric dipoles in the polymer chain. Interaction between PVDF and nanoparticles should straighten the PVDF backbone, leading to the transformation of α-polymorph to the β-polymorph [11].

3.3 XRD

X-ray diffraction patterns of pure PVDF and its nanocomposites were shown in Fig. 5. The pure PVDF exhibits peaks at 17.8, 18.6, 19.96, and 26.6 characteristic of α-polymorph [6]. No appreciable change has been found at PVDF/0.1% Cu as compared to pure PVDF spectrum. The

significant changes in the crystal structure of the polymer phase were observed after the inclusion of 1 wt% of Cu-NPs in the polymer. In the PVDF/1% Cu, the peak at 26.6 disappears and the peak at 19.96 shifted to 20.3 corresponding to β-phase and assigned to the reflection of (110)/(200) planes [22]. In general, appearance of a major peak higher than $2\theta = 20°$ along with no peak at $2\theta = 26°$ is clear evidence for formation of higher β-polymorph content inside the polymer matrix [17]. The diffraction peaks at 43.5 and 50.4 correspond to (111) and (200) planes of fcc structure of copper [23], and are only observed for nanocomposites with a Cu percentage higher than 0.1%.

3.4 SEM

SEM images of the surface of pure PVDF and PVDF/Cu nanocomposites are shown in Fig. 6. SEM micrographs show spherulitic crystal structure of PVDF; the size of the spherulites is about 20 μm. The spherulitic crystallization morphology of the pure PVDF is maintained for the PVDF nanocomposites. The size of these spherulites decreased with the further increase of Cu-NPs content to about 6 μm.

3.5 UV–Visible Characterization

The UV–Vis spectra of colloidal Cu-NPs synthesized in water and PVDF/Cu nanocomposites were shown in Fig. 7a and b, respectively. The absorption bands for Cu-NPs have been reported to be in the range of 500–600 nm [23]. Fig. 7a shows a surface plasmon resonance (SPR) band centered around 577 nm. In the UV–Visible spectrum of nanocomposites no absorption in the visible range was
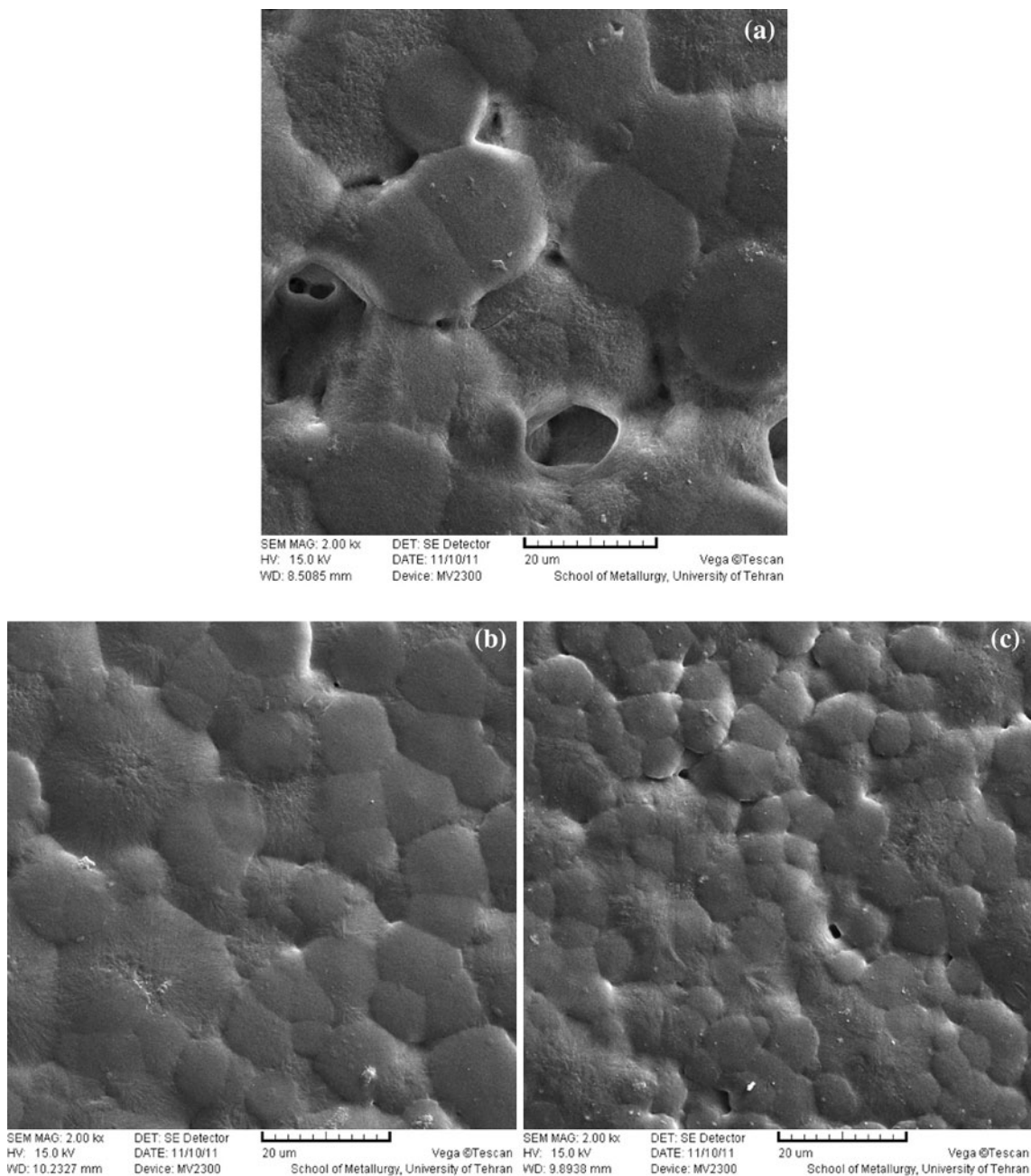
Fig. 6 SEM images of: **a** pure PVDF, **b** PVDF/0.1% Cu and **c** PVDF/1% Cu

observed (Fig. 7b). This is may be due to the intense scattering by the composites, which is intense, and therefore completely masks the SPR band of Cu [16].

In order to study the effect of embedding of Cu-NPs on the optical transition behavior of PVDF, optical band gap (E_g) for pure PVDF and its nanocomposite films has been determined using Tauc's relation [24]:

$$(\alpha hv)^{\frac{1}{2}} = B(hv - E_g) \tag{2}$$

where α is the absorption coefficient, hv is the photon energy and B is the constant of proportionality. The

values of E_g can be deduced from the intercept of the linear fitted lines in the plots of $(\alpha hv)^{1/2}$ versus hv, as shown in Fig. 8.

The values of E_g are listed in Table 1. It is obvious that the value of E_g decreases from 4.90 eV for pure PVDF to 3.2 eV for PVDF/1%Cu nanocomposite. Such a decrease in the value of E_g can be attributed to the formation of trap levels between the highest occupied molecular orbital (HOMO) and unoccupied molecular orbital (LUMO) energy states. The presence of the nanoparticles introduce many states into the polymer's HOMO–LUMO gap,

Fig. 7 UV–Visible absorption spectrums of: **a** the Cu-NPs dispersed in water and **b** pure PVDF and nanocomposite films
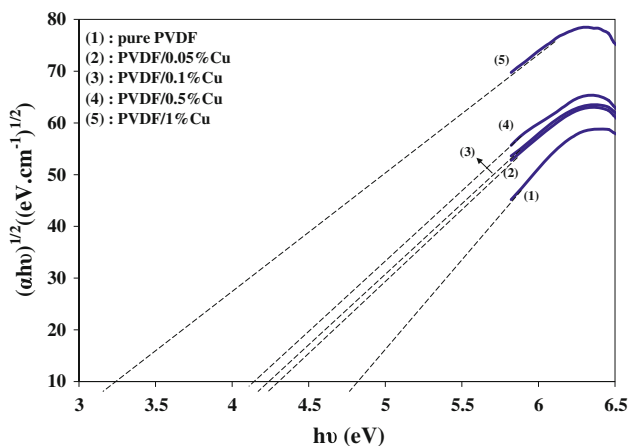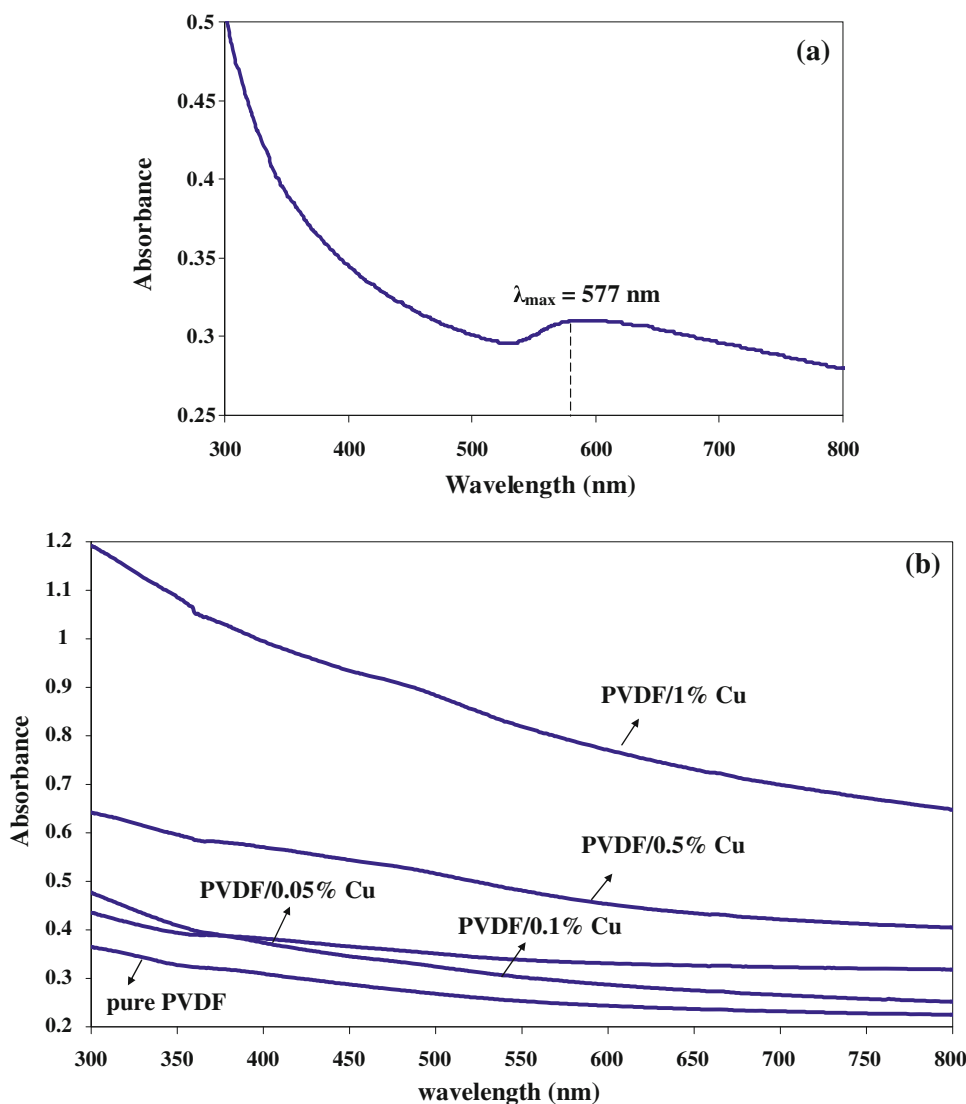
Fig. 8 Plots of $(\alpha h\upsilon)^{1/2}$ versus $(h\upsilon)$ for pure PVDF and PVDF/Cu nanocomposite films

making the lower energy transitions possible and results in the reduction of optical band gap[25].

3.6 TGA

Thermal stability of the nanocomposites was studied by TGA. Figure 9 shows the TGA thermograms of pure PVDF and PVDF/Cu nanocomposite films. The thermo-degradation of PVDF is observed around 409 °C (determined from the first inflection point of the curve). By the addition of Cu-NPs, the degradation temperature increases to 421 and 430 °C for the PVDF/0.1% Cu and PVDF/1% Cu, respectively. Indeed, only the 1 wt% Cu-NPs causes an increase of degradation temperature of 21 °C. Therefore, the presence of the Cu-NPs modifies the thermal stability of the polymer matrix. The resistance of nanocomposites toward thermal degradation may be related to the

Table 1 Optical band gap for pure PVDF and PVDF/Cu nanocomposite films

Sample	Optical band gap (eV)
PVDF	4.77
PVDF/0/05% Cu	4.3
PVDF/0/1% Cu	4.12
PVDF/0/5% Cu	3.4
PVDF/1% Cu	3.2
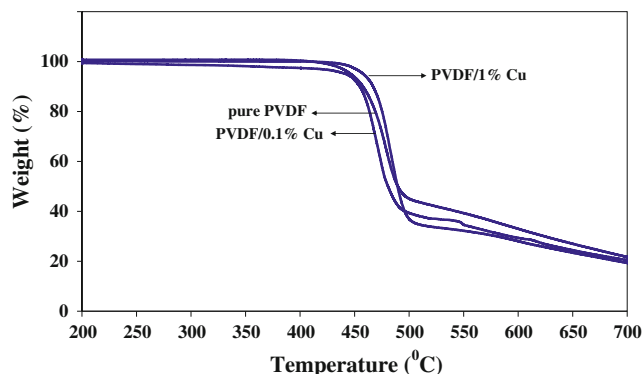
Fig. 9 TGA thermograms of pure PVDF and PVDF/Cu nanocomposite films

Table 2 Resistivity (ρ) for pure PVDF and PVDF/Cu nanocomposite films

Sample	Resistivity (Ωcm)
PVDF	3×10^6
PVDF/0/05% Cu	2.4×10^6
PVDF/0/1% Cu	1.8×10^6
PVDF/0/5% Cu	1.4×10^6
PVDF/1% Cu	8×10^5

interaction between PVDF and Cu-NPs. The strong interaction between nanoparticles and the PVDF matrix is indicated by the FT-IR spectra and XRD patterns too.

3.7 Resistivity

The resistivity of the samples was measured by an electrometer using a two-probe method. In this method two electrodes are attached to the sample in order to measure the resistance and from the information of the sample geometry, the resistivity can be determined using the following equation [26]:

$$\rho = \frac{RA}{l} \tag{3}$$

where l is the thickness and A is the area and R is the resistance of the sample. The resistivities of PVDF/Cu

nanocomposite films and the pure PVDF film were calculated, based on Eq. 3 and are presented in Table 2. These data shows that the resistivity decreases therefore the conductivity improves with increasing Cu-NPs concentration.

4 Conclusions

The PVDF/Cu nanocomposites were prepared by mixing of Cu-NPs in DMF and PVDF solution. The nanocomposite films were studied by various methods. The results of FTIR exhibited the polymorph transformation from α- to β-phase as a result of insertion of Cu-NPs. This conclusion was supported by XRD data. The polymorph change induced by the dipole interaction between C–F band of PVDF and the Cu-NPs. Thermal stability of the PVDF was improved by the addition of the Cu-NPs. The higher thermal stability of PVDF nanocomposite supports our assumption of polymorph change in the polymer. This happens because of the β-phase has a higher thermal stability due to the better packing than that of the α-PVDF. The PVDF resistivity decreases with increase in Cu-NPs concentration.

References

1. E. Fukada, IEEE Trans. Ultrason. Ferroelectr. Freq. Control **47**, 6 (2000)
2. A.V. Shirinov, W.K. Schomburg, Sens. Actuators A **142** (2008)
3. P. Ueberschlag, Sens. Rev. **21**, 6 (2001)
4. C. Chandrana, J. Talman, T. Pan, S. Roy, A. Fleischman, Sensors **10** (2010)
5. A. Samili, A.A. Yousefi, J. Polym. Sci. **42** (2004)
6. B. Mohammadi, A.A. Yousefi, S. Moemen Bellah, Polym. Test. **26** (2007)
7. S. Lanceros-Me′ndez, J.F. Mano, A.M. Costa, V.H. Schmidt, J. Macromol. Sci. Phys. **40** (2001)
8. Y.J. Park, Y.S. Kang, C. Park, Eur. Polym. J. **41** (2005)
9. D. Dasgupta, S. Manna, A. Garai, A. Dawn, C. Rochas, J.M. Guenet, A.K. Nandi, Macromolecules **41** (2008)
10. Y. Bormashenko, R. Pogreb, O. Stanevsky, E. Bormashenko, Polym. Test. **23** (2004)
11. A.A. Yousefi, Iran. Polym. J. **20**, 9 (2011)
12. K. Wang, H. Lee, R. Cooper, H. Liang, Appl Phys A **95** (2009)
13. Q.Y. Peng, P.H. Cong, X.J. Liu, T.X. Liu, S. Huang, T.S. Li, Wear **26**(7–8) (2009)
14. J. Yu, P. Jiang, C. Wu, L. Wang, X. Wu, Polym. Compos. **32**, 10 (2011)
15. L. He, Q. Xu, C. Hue, R. Song, Polym. Compos. **31**, 5 (2010)
16. D. Miranda1, V. Sencadas, A.S. Iglesias, I.P. Santos, L.M. LizMarzán, J.L. Gómez Ribelles, S.L. Mendez, J. Nanosci. Nanotechnol. **9** (2008)
17. W. Wang, S. Zhang, L. Srisombat, T. Randall Lee, R.C. Advincula, Macromol. Mater. Eng. **296** (2011)
18. R. Lin, L. Fang, X. Li, Y. Xi, S. Zhang, Polym. Int. **55** (2006)
19. V.H. Poblete, M.P. A'lvarez, V.M. Fuenzalida, Polym. Compos. **30** (2008)
20. I.B. Jeong, Y.S. Kim, B.Y. Lee, Y.H. Kim, B.S. Jeong, M.S. Lee, Patent Application Publication Pub. No.: US 2004/0221685A1 (2004)

21. G. Zhao, M.P. Pompeo, Patent Application Publication Pub. No.: US 7517382B2 (2009)
22. W. Ma, J. Zhang, X. Wang, J. Mater. Sci. **43** (2008)
23. T.M. Dung Dang, T.T. Tuyet Le, E.F. Blanc, M.C. Dang, Adv. Nat. Sci. Nanosci. Nanotechnol. **2** (2011)
24. R. Chahal, S. Mahendia, A.K. Tomar, S. Kumar, Dig. J. Nanomaterials Biostructures **6** (2011)
25. S. Mahendia, A.K. Tomar, R. Pal Chahal, P. Goyal, S. Kumar, J. Phys. D **44** (2011)
26. R.K. Layek, S. Samanta, D.P. Chatterjee, A.K. Nandi, Polymer **51** (2010)